

Molecular Orbital Approach to Chemisorption. II. Atomic H, C, N, O, and F on Graphite

Alan J. Bennett, Bruce McCarroll, and Richard P. Messmer

General Electric Research and Development Center, Schenectady, New York 12301

(Received 13 August 1970)

The calculation of the chemisorption behavior of atomic H, C, N, O, and F on a graphite basal (0001) surface is examined with the CNDO (complete neglect of differential overlap) molecular-orbital scheme. This approach is a semiempirical approximation to the Hartree-Fock self-consistent field procedure, in which the Hamiltonian explicitly depends upon both atomic and orbital charge distribution. The location of binding sites and changes in relative binding energies and net charges with the identity of the adsorbed species are explored with an extended carbon (0001) surface, simulated by an 18-carbon lattice with appropriate boundary connections. The strength of binding to the simulated graphite substrate increases in the order H, F, O, N, and C. The atoms C and N are most stable when positioned above the center of a hexagonal six-carbon ring, whereas H, F, and O are most stable above the center of a bond connecting nearest-neighbor carbons. Calculated charge distributions are used to predict a work-function decrease with the adsorption of atomic H or N on graphite, but an increase with the adsorption of C, O, or F. The commonly used electronegativity reasoning is shown to be inadequate for the prediction of adsorbate-charge transfer.

I. INTRODUCTION

In a previous paper (I),¹ we began an investigation of the application of a simple molecular-orbital (MO) theory to the understanding of chemisorption phenomena.² The object of these studies is to achieve a semiquantitative self-consistent quantum description of both the bulk and surface properties of the substrate using the simplest adequate MO description.³ Semiempirical MO methods invariably fail to predict the correct absolute magnitude of molecular binding energies, but do yield good relative binding energies which are of great interest in the interpretation of chemisorption experiments.

An extended Hückel theory (EHT) was applied to the graphite-adsorbate system in I. The substrate was represented by a finite number of atoms which described the effect of surface-lattice geometry. The EHT is a semiempirical MO scheme in which diagonal elements of the Hamiltonian matrix in a Slater-orbital basis are set equal to ionization potentials. Off-diagonal elements are set proportional to the product of the average of the two relevant atomic ionization potentials and the overlap integral of the relevant atomic orbitals. The binding energy is calculated as the difference between the sum of the molecular one-electron energies and the sum of one-electron energies of the separated constituent atoms. No explicit account is taken of either electron-electron or core-core interactions between atoms. Consequently, the Hamiltonian matrix elements in the original formulation are not parametrically dependent upon charge distribution in the molecule. Later modifications include some such self-consistent effects.

In I only those matrix elements associated with the adsorbate were iteratively adjusted. The calculations yielded a semiquantitative description of the bare graphite substrate (bandwidths and cohesive energy) and the binding behavior of adsorbed hydrogen. In particular, the dependence of binding energy on adsorbate position and the concomitant charge transfer (0.2 electrons) from the hydrogen to the substrate were obtained.

Similar EHT calculations for the electrophilic adsorbates C, O, and N were less encouraging. Self-consistent adjustment of adsorbate energy levels was inadequate to obtain convergence. Large physically unreasonable charge transfers of two electrons frequently occurred. Subsequent attempts to improve the results by self-consistent adjustment of all matrix elements failed: The EHT calculation of the adsorption energy still yielded unphysical binding curves in which binding catastrophically increases with separation, and no stable adsorbate position exists.

Rather than further modify the EHT in an *ad hoc* manner, we explore the application of a more sophisticated MO procedure, the complete-neglect-of-differential-overlap scheme (CNDO) developed by Pople and his collaborators.⁸⁻¹² The Hamiltonian matrix elements and calculation of binding energy within this scheme explicitly include the electron-electron and core-core interaction between atoms. These effects tend to control the charge transfer and yield physically reasonable binding curves. Even with the neglect of these additional interactions, the CNDO parametrization is different and thus not comparable to the EHT parametrization. Correlation of the experimental value of the cohesive energy of the graphite lattice with that pre-

dicted by the two methods is useful for scaling the calculated energies because the absolute values of binding energies obtained with these methods are known to be consistently too large.

In I we found that a two-dimensional 16-carbon representation of the graphite substrate was reasonably adequate for obtaining relative binding energies. The use of a finite representation replaces integrals over k space with finite sums: For reasonably smooth energy bands, little error is made by this replacement.

The atoms on the perimeter of the representation had, however, incompletely occupied orbitals. As a result, two classes of electron states were obtained; band states which extend throughout the representation and localized states confined to the perimeter. The representation thus approximated a plateau region on a substrate formed, for example, by adsorbate reactions which remove surface atoms. Interactions with a perfect surface were approximated by placing adsorbates near the center of the representation and experimentally interesting interactions with edges were approximated by placing adsorbates near the perimeter.

Periodic boundary conditions are necessary in simulating perfect surfaces. Therefore, in the present work the surface is simulated by a connected array of finite representations. The edge states thus are eliminated. A single adsorbate atom above the representation is then equivalent to a periodic planar array of adsorbate atoms analogous to those observed in low-energy-electron-diffraction (LEED) experiments with adsorbed layers. If only one adsorbate atom is placed on the representation, the spacing between members of this periodic array of atoms is large. The periodic connectivity conditions then serve only to eliminate the undesired edge states which can often affect the adsorbate interaction.

The CNDO approximation is discussed in Sec. IIA together with a description of the convergence criteria used (Sec. IIB) and a description of the periodic connectivity conditions (Sec. IIC). In Sec. III are results for the binding energies and charge distributions associated with atomic H, C, N, O, and F chemisorbed on graphite. The examination of various overlap populations permits a discussion of adatom binding to the surface in terms of the more conventional visualizations of chemical binding used for small molecules.

II. METHOD OF CALCULATION

A. CNDO Approximation

The CNDO method has been developed in a series of papers by Pople and his collaborators.⁸⁻¹² Their aim was to provide a useful approximation to the Hartree-Fock equations for the treatment of all

valence electrons by explicit inclusion of electron and core interactions. A recent text fully describes this approach.¹² Here we briefly review its basic approximations and the formulas used in the calculations.

The wave functions are antisymmetrized products of one-electron spin orbitals ϕ_i^γ which are taken as

$$\phi_i^\gamma(r, s) = \sum_{\lambda} C_{i\lambda}^\gamma \chi_{\lambda}(r) v_{\gamma}(s), \quad (2.1)$$

where the χ_{λ} are real Slater orbitals centered on the atoms of the system, and $v_{\alpha}(s) = \alpha(s)$ and $v_{\beta}(s) = \beta(s)$. The real coefficients $C_{i\lambda}^\gamma$ and eigenvalues E_i are then determined⁹ by solution of

$$\|F_{\lambda\sigma}^\gamma - E^\gamma S_{\lambda\sigma}\| = 0, \quad (2.2)$$

where S is the overlap matrix associated with the $\{\chi\}$, and

$$F_{\lambda\sigma} = F_{\lambda\sigma}^\alpha + F_{\lambda\sigma}^\beta. \quad (2.3)$$

The separation of the Hartree-Fock Hamiltonian F into one-electron and two-electron terms proves convenient:

$$F_{\lambda\sigma}^\gamma = H_{\lambda\sigma}^\gamma + G_{\lambda\sigma}^\gamma, \quad (2.4)$$

with

$$H_{\lambda\sigma}^\gamma = \langle \lambda | -\frac{1}{2} \nabla^2 - \sum_A Z_A / (r - R_A) | \sigma \rangle, \quad (2.5)$$

$$G_{\lambda\sigma}^\gamma = 2 \sum_{\mu\nu} P_{\mu\nu}^\gamma \langle \lambda\sigma | \mu\nu \rangle - \sum_{\mu\nu} P_{\mu\nu}^\gamma \langle \mu\sigma | \lambda\nu \rangle. \quad (2.6)$$

The density matrices are given by

$$P_{\mu\nu}^\gamma = \sum_i C_{i\mu}^\gamma C_{i\nu}^\gamma, \quad (2.7)$$

where i is an occupied state with

$$P_{\mu\nu} = P_{\mu\nu}^\alpha + P_{\mu\nu}^\beta, \quad (2.8)$$

and the charge on an atom A is given by

$$P_{AA} = \sum_{\mu}^A P_{\mu\mu}. \quad (2.9)$$

The quantities Z_A and R_A are the core charge and nuclear position of atom A , respectively.

The approximations consist of (a) ignoring differential overlap between nonorthogonal atomic orbitals (the CNDO approximation), i.e., the S_{ij} in Eq. (2.2) and the Coulomb integrals $\langle \lambda\sigma | \mu\nu \rangle$ other than those of the form $\langle \lambda\lambda | \mu\mu \rangle$; (b) demanding rotational invariance by replacing certain integrals with values characteristic of s orbitals on the atomic species A and B and of the interatomic separation:

$$\langle \lambda^A \lambda^A | \mu^B \mu^B \rangle = \gamma_{AB}$$

and

$$\langle \mu^A | Z_B / (r - R_B) | \mu^A \rangle = V_{BA};$$

(c) setting

$$\langle \lambda | -\frac{1}{2} \nabla^2 - Z_A / (r - R_A) | \lambda \rangle = -\frac{1}{2} (I_{\lambda} + A_{\lambda}) - Z_A - \frac{1}{2} \gamma_{AA},$$

where I_{λ} and A_{λ} are the valence-state ionization

potential and electron affinity of the λ atomic orbital; (d) setting

$$\langle \lambda | -\frac{1}{2} \nabla^2 - \sum_A Z_A / (r - R_A) | \mu \rangle = -\frac{1}{2} (\beta_A + \beta_B) S_{\lambda\mu},$$

where the β 's are determined by comparison with full SCF (self-consistent field) calculations for diatomic molecules; and (e) assuming that $Z_A \gamma_{BA} = V_{BA}$.

The values of β_A given by Pople *et al.* are often well approximated by $1.5 \bar{I}_A$, where \bar{I}_A is an average ionization potential for the atom. A comparison of the off-diagonal Hamiltonian matrix elements of the EHT shows that this identification ensures that the general bandwidth obtained by the two methods be similar.

Use of the above approximations yields the standard CNDO/2 expressions¹⁰ for the matrix elements of $F = H + G$:

$$H_{\mu\mu}^{\gamma} = -\frac{1}{2} (\bar{I}_{\mu} + A_{\mu}) - (Z_A - \frac{1}{2}) \gamma_{AA}, \quad (2.10)$$

$$G_{\mu\mu}^{\gamma} = \sum_{B \neq A} (P_{BB} - Z_B) \gamma_{AB} + (P_{AA} - P_{\mu\mu}^{\gamma}) \gamma_{AA}, \quad (2.11)$$

$$H_{\mu\nu}^{\gamma} = -\frac{1}{2} (\beta_A + \beta_B) S_{\mu\nu}, \quad (2.12)$$

$$G_{\mu\nu}^{\gamma} = -P_{\mu\nu}^{\gamma} \gamma_{AB}. \quad (2.13)$$

After iteration to convergence (discussed below), the net binding energy of the system is determined from

$$E = \frac{1}{2} \sum_{\mu\nu} P_{\mu\nu} (H_{\mu\nu} + F_{\mu\nu}) + \sum_{A < B} \frac{Z_A Z_B}{R_{AB}} - \frac{1}{2} \sum_A \sum_{\lambda, \nu}^{\text{atom}} P_{\lambda\nu} (H_{\lambda\nu} + F_{\lambda\nu}), \quad (2.14)$$

where the last sum accounts for the separated constituent atoms. A negative value of E implies a bound system.

Electron distributions and their role in the formation of chemical bonds between the adsorbate and the substrate can be investigated through the use of overlap populations such as described by Mulliken.¹³ Similar to these we use an orbital overlap population $n(\mu, \nu)$ between atomic orbitals μ on atom A and ν on atom B ,

$$n(\mu, \nu) = (2 - \delta_{AB}) P_{\mu\nu} S_{\mu\nu}. \quad (2.15)$$

From these the atomic overlap population between atom A and B can be formed,

$$n(A, B) = \sum_{\mu}^A \sum_{\nu}^B n(\mu, \nu). \quad (2.16)$$

This quantity is a measure of the chemical bonding between the two atoms.

We also need the overlap population between an adsorbed atom A and the substrate

$$n(A) = \sum_{B \neq A} n(A, B). \quad (2.17)$$

This estimate of the degree of binding between the

adatom and the substrate facilitates comparison with binding of this atom in simple compounds in which the behavior is better understood.

There are two main advantages to this CNDO/2 approach.¹⁰ First, this SCF scheme is sensitive to both the atomic and orbital charge distributions through specific inclusion of electron-electron interaction terms. This, as is mentioned in the Introduction, is what is believed necessary to ameliorate the unrealistic charge redistributions encountered upon using EHT to describe the interactions of an electrophilic adsorbate with graphite. Second, parameters for the atoms comprising the systems of immediate interest are available.⁸⁻¹⁰ These are reproduced in Table I for convenience. Adjustment of these parameters to account for the changes in screening associated with the solid state will be examined in future work.

Two modifications of the standard procedure¹⁴ are made. One is needed to overcome an interesting data-sensitive instability. The other permits the imposition of periodic boundary connections on the 18-carbon representation of the surface.

B. Convergence of Computations

A CNDO/2 calculation is started by the use of an extended Hückel-like calculation to obtain initial eigenvectors. These starting eigenvectors are used to form the P matrix which is in turn used to form the F matrix of Eq. (2.3). The next estimate of the eigenvectors is obtained by diagonalization of F , and so on. Convergence is obtained when the energies calculated by two successive iterations satisfy

$$| (E^{(n+1)} - E^{(n)}) / E^{(n)} | < 2 \times 10^{-6}.$$

Under what is here defined as normal circumstances, $E^{(n+1)} < E^{(n)}$. However, for reasons not completely understood, some calculations behaved in a manner similar to that described by Ransil¹⁵ for certain diatomics. His calculated energy did not converge, but instead alternated on successive iterations between two distinct values.

In some of our calculations there was an initial approach to convergence, followed by an alternation between two energies, both of which are more positive than the last energy prior to oscillation. Analysis of the $P_{\mu\nu}^{\gamma}$ and atomic charge distributions of

TABLE I. Parameters used in the CNDO/2 calculations.^a

Atom	H	C	N	O	F
$\frac{1}{2} (I_s + A_s)$ (eV)	7.176	14.051	19.316	25.390	32.272
$\frac{1}{2} (I_p + A_p)$ (eV)	...	5.572	7.275	9.111	11.080
$-\beta_A$ (eV)	9	21	25	31	39
Slater exponent	1.20	1.62	1.95	2.27	2.60

^aReferences 9 and 10.

these calculations revealed that (i) in the lowest energy mode, atomic and orbital charge distributions are normal in that they reflected the symmetry imposed by lattice and orbital geometry, (ii) in the other two modes, an unacceptable pathology clearly exists; they corresponded to two variants of charge piling up on alternate atoms, leaving the remainder devoid of valence electrons. These two systems are not bound. Sometimes a slight change of $\pm 0.1 \text{ \AA}$ in the height of an adsorbate atom yields a normal calculation, but the threat of such unpredictable pathology is unacceptable for extended calculations.

This behavior is eliminated through the estimation of a new approximation to the density matrix $P_{\mu\nu}^y$ if the system appears to be going out of bounds. The normal calculation sequence is depicted by

$$\{C\}^{(n)} \rightarrow P^{(n)} \rightarrow F^{(n+1)}, E^{(n)} \rightarrow \{C\}^{(n+1)},$$

where n designates the iteration. However, assume that $E^{(n+1)} > E^{(n)}$, but $E^{(n)} < E^{(n-1)}$. This behavior in the electronic energy implies that the matrices $P^{(n+1)}$ give a bad Hamiltonian matrix $F^{(n+2)}$ which yields a bad $P^{(n+2)}$, etc. New density matrices are estimated by

$$P'^{(n+1)} = \epsilon P^{(n)} + (1 - \epsilon) P^{(n+1)}$$

and the new $E'^{(n+1)}$ is calculated from the $F'^{(n+2)}$. If $E'^{(n+1)} < E^{(n)}$ the calculation then proceeded in the normal manner. If $E'^{(n+1)} > E^{(n)}$ still, then estimates with a smaller ϵ are made until normal behavior is obtained. A starting value of $\epsilon = 0.8$ is taken and smaller values are obtained by the substitutions $\epsilon \rightarrow 0.8\epsilon$, if needed.

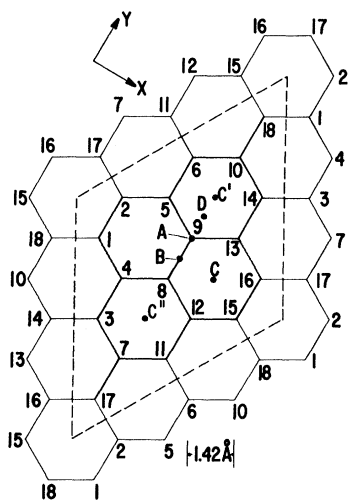


FIG. 1. Schematic of the 18-C representation for a graphite (0001) surface. C atoms are located at vertices, and labeled points denote lattice positions over which adsorbate atoms are placed. Periodic connections are indicated (see text, Sec. II C).

The need for this restarting varies considerably between calculations; some need it not at all. If there is a restart, then the energy convergence criterion is modified to

$$|(E'^{(n+1)} - E^{(n)})/\epsilon E^{(n)}| < 2 \times 10^{-6}$$

to allow for smaller energy differences between iterations.

This procedure can certainly be criticized on the grounds that there is no obvious guarantee that a wave function exists that corresponds to the interpolated matrix. Such a situation can lead to conceptual difficulties within the framework of an SCF calculation.

In defense of the procedure, however, a series of calculations of binding energies and charge distributions as a function of adsorbate-substrate distance yield results which are points on smooth curves. The points obtained from calculations that do require restarts cannot be discerned from the points obtained from those that do not. Other quantities of interest also behave in a regular manner.

C. Periodic Connectivity Conditions

Our simulation of the interaction of a gas atom with an infinite surface involves a finite representation of the surface. To remove the edge states mentioned in the Introduction, the edge atoms of the representation must be suitably connected to other carbon atoms.

The most convenient scheme and the one used to construct the Hamiltonian matrix for the calculations reported herein consists first of allowing all pairs of the 18 atoms in the representation to interact. This 18-carbon representation is contained in a cell that consists of a 3×3 block of unit cells of two atoms each (Fig. 1). The interactions between atoms in the cell and those outside are then used to replace their weaker analog within the cell. For example, carbon 1 and carbon 18 interact as nearest neighbors, carbon 1 and carbon 16 as next-to-next-nearest neighbors. The adsorbate interacts only with the atoms in the cell.

The suitability of this scheme for the simulation of an extended surface is demonstrated in Sec. III where it is shown that the charge densities obtained for the bare lattice are suitably uniform and that adsorbate binding curves exhibit small deviations at positions that would be exactly equivalent with the perfect periodicity. Use of standard CNDO parameters show that the relevant interatomic overlaps decrease very rapidly with distance and so for systems exhibiting small ionicity, this behavior is not surprising.

III. RESULTS AND DISCUSSION

In order to determine the effect of the periodic connections, some comparisons are first made be-

TABLE II. Distribution of valence electrons on substrate lattices.

Atom	CNDO/2			EHT
	18-C connected	18 C	16C	16C
2	4.00	4.05	4.09	4.27
5	4.00	3.97	3.91	3.65
6	4.00	4.00	4.05	4.19
9	3.99	4.05	4.06	3.78
10	4.00	3.89	3.83	4.00
18	4.01	4.03

tween results for the periodically connected 18-carbon lattice and those obtained with the CNDO approximation on the 16-carbon lattice introduced in I and given by atoms 1-16 in Fig. 1. In addition, the CNDO results for the bare substrate and hydrogen adsorption are compared with the analogous results obtained in I with the EHT on the 16-carbon representation.

A. Graphite Substrate

The valence charge distributions calculated for the various models of the bare graphite lattice are summarized in Table II, which should be used in conjunction with Fig. 1. A comparison of the last two columns strikingly demonstrates the effects of a calculation that explicitly considers atomic and orbital charge distribution (CNDO) and one that does not (EHT). The large deviations from neutrality calculated with the EHT are considerably reduced with the CNDO treatment.

A feeling for the effects of the boundary connections on the charge distributions is obtained from a comparison of the two 18-carbon columns. These results of CNDO calculations indicate that a further smoothing of the charge distribution is achieved with the connections. The small charge deviations that remain for the connected lattice reflect our neglect of longer-range interactions across the boundary of the representation. Adatom binding can also be influenced by the presence of the boundary connections. This is examined below.

The stability of the connected representation is demonstrated by a plot (Fig. 2) of the calculated cohesive energy [net binding energy, Eq. (2.14)] of the 18-carbon connected lattice as a function of nearest-neighbor spacing. Maximum lattice stability is achieved at a spacing of $\sim 1.4 \text{ \AA}$ which is the experimentally observed value for graphite.

The cohesive energy (the negative of the binding energy) is calculated to be 26.33 eV per atom for the periodically connected 18-carbon lattice. For the 16-carbon representation of I, where there are fewer bonds, a CNDO calculation yields 21.85 eV per atom. These values are much higher than the experimental value of $\sim 5 \text{ eV}$ ¹⁶ and the EHT value

of $\sim 4.16 \text{ eV}$ for the 16-carbon representation (I).

CNDO calculations consistently yield binding energies larger than the experimental values. However, preliminary results¹⁷ indicate that the inclusion of the S_{ij} in Eq. (2.2), as is usual in EHT calculations but neglected in the first approximation of Sec. IIA, lowers the calculated values.

The values of the cohesive energy suggest that a reasonable approximation consists of scaling down the CNDO calculated binding energies by a factor of ~ 5 for comparison with experiment. Comparison below of EHT and CNDO hydrogen-adsorption calculations supports this observation.

The work function obtained by the CNDO calculation is 6.36 eV as compared to $\sim 10.1 \text{ eV}$ obtained with the EHT and the measured value of $\sim 4.8 \text{ eV}$.¹⁸ It should be noted that the CNDO calculation indicates an occupied bandwidth about three times greater than that predicted by the extended Hückel approximation and experiment.¹⁹

B. Chemisorption

1. Charges and Work-Function Changes

In the Introduction it was noted that the EHT fails catastrophically when applied to systems with electrophilic adsorbates. The calculated (CNDO) behavior of the net charge on a nitrogen atom as a function of its distance above an 18-carbon periodically connected lattice is shown in Fig. 3. This calculation, which specifically includes electron-electron interactions, demonstrates that such effects are a vital ingredient in a MO description of adsorption. Other electrophilic adsorbates behave similarly: Close to the surface the adatom transfers charge into the lattice, but as the distance from the surface increases the adatom accumulates charge in excess of the neutral value. At separations greater than $\sim 1.5 \text{ \AA}$ the simple MO approach becomes inadequate and the inclusion of configuration interaction is required.

The behavior of the charges on adatoms located over the lettered positions on the substrate (Fig. 1) is summarized in Table III. The valence charges

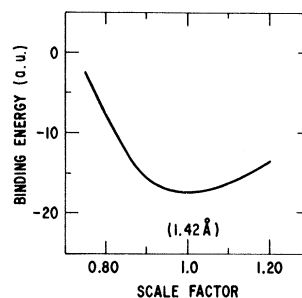


FIG. 2. Binding energy (Hartree) of the 18-C lattice with periodic connections as the C-C spacing is varied.

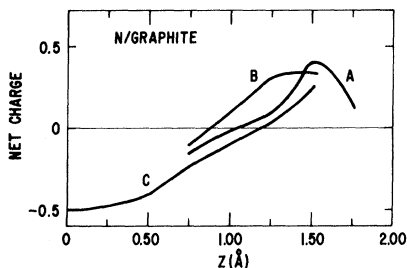


FIG. 3. Net charge calculated for a nitrogen adatom placed over the 18-C periodically connected lattice in the lettered positions indicated (Fig. 1). The Z direction is perpendicular to the plane of the graphite representation.

shown are for the adatom located at a distance for which there is a minimum in the plot of binding energy vs distance above the lattice (Sec. III B 2). There are no extreme charge deviations from neutral adatom values.

Experimentally observed changes in the work function that can occur upon adsorption of gases on solids are customarily ascribed²⁰ to changes in the effective surface dipole moment. Positive dipoles correspond to excess positive charge on the adatom which causes a work-function decrease.

The dipole moment can, in principle, be obtained from the calculated wave functions. Here, estimates of the sign of the work-function changes upon adsorption are made from the net atomic charges of Table III: On adsorption at the most stable binding positions, hydrogen or nitrogen atoms should yield work-function decreases. Adsorption of carbon, oxygen, or fluorine atoms should yield work-function increases as is expected for the chemisorption of species whose electronegativity exceeds that of the substrate.

Estimates of work-function changes based on simple electronegativity considerations are often used.²¹ The calculated behavior of nitrogen on graphite reinforces the view²⁰ that differences in electronegativity between the substrate and the adatom are not a reliable guide to predicting the effects of adsorption. Estimating the surface electronegativity X_M (Pauling scale) of the 18-carbon lattice, for example, from²¹

$$X_M = 0.335 \varphi_m$$

gives 2.2 for the surface electronegativity using the calculated work function of 6.62 eV. Use of the experimental value¹⁸ of ~ 4.8 eV gives a surface electronegativity of 1.6.

A comparison of the electronegativity of a nitrogen atom ($X_N = 3.0$) with the surface electronegativities estimated for the lattice predicts charge accumulation on the adatom, with a concomitant work-function increase. However, the opposite is

predicted by the charge densities calculated for nitrogen above point C. The results of these calculations suggest that (a) simple electronegativity arguments are not reliable for the prediction of adsorbate charge transfer and (b) the adsorbate charge transfer is sensitive not only to the particular crystal plane, but also to the precise location of the binding site on a given plane.

2. Binding Sites

The adsorbate binding energy E_B which is best considered as the relative binding strength of an adatom to a substrate site is obtained from

$$E_B = E_{\text{total}}(\text{lattice} + \text{adatom}) - E_{\text{total}}(\text{lattice}) \\ - E_{\text{total}}(\text{adatom at } \infty),$$

where "lattice" refers to the 18-carbon connected representation unless otherwise noted. It is anticipated that a scaling down of calculated E_B by a factor of 4 or 5 should provide estimates of the experimental magnitudes.

The ability to predict sites of strongest adatom binding is cardinal to any chemisorption theory. Potential scans of the surface representation with the adatom as a probe are usually prohibitively expensive, although they were obtained for the hydrogen-atom-graphite system¹ and do give an elegant picture of the energetics of the interaction. An alternate procedure is to select points of high symmetry on the lattice and calculate the adatom binding energy E_B as a function of distance Z above these points.

The results of such CNDO/2 calculations are displayed in Figs. 4–8 for H, C, N, O, and F atoms on the 18-carbon connected representation: They display an encouraging sensitivity to the chemical identity of the adatom and to its location on the surface representation.

To briefly summarize, listed in order of increasing binding energies are H, F, O, N, and C. Grouped according to binding sites, C and N appear to be most stable above the center of a hexagon (point C, Fig. 1), whereas H, O, and F find maxi-

TABLE III. Adsorbate valence charge at binding minima on 18-carbon connected lattice.

Atom	Position ^a				∞^b
	A	B	C	D	
H	0.962	<u>0.858</u>	0.413	0.849	1.00
C	4.02	4.03	<u>4.02</u>	4.06	4.00
N	5.08	5.31	<u>4.78</u>	5.16	5.00
O	6.40	<u>6.25</u>	6.19	6.24	6.00
F	7.27	<u>7.09</u>	7.41	7.15	7.00

^aUnderlined values designate most stable binding positions.

^bNumber of valence electrons.

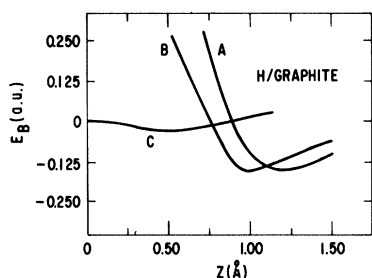


FIG. 4. Binding energy of a hydrogen adatom (Hartree) as a function of the distance Z above the labeled positions on the 18-C periodically connected lattice.

imum stability above the center of a bond connecting nearest-neighbor carbons (point B, Fig. 1).

The behavior of oxygen above points B and D is noteworthy, and is to be contrasted with the behavior of H and of F above these points. Although these three atoms bind most strongly over position B in a bridged configuration, oxygen atoms possess a secondary bridge position at D which is suggested by the energetics shown in Fig. 7. The oxygen sites in order of decreasing binding energy are B, D, A, and C. However, hydrogen and fluorine sense stability in the decreasing order B, A, D, and C. The physical implications of these energetics is that hydrogen and fluorine atoms probably migrate above the C - C bonds, but oxygen atoms migrate along a path that avoids carbon atoms (type-A sites) and the centers of the hexagons (type-C sites).

Note that the present CNDO calculations for hydrogen atoms on an 18-carbon connected lattice predict the position of maximum binding for hydrogen atoms to be above a C - C bond. Our earlier¹ EHT calculation for hydrogen atoms on a 16-carbon sheet (with no attempt at periodic boundary conditions) indicated maximum stability for the hydrogen atom directly above a lattice carbon atom. This difference is due to the periodic connections used for the 18-carbon representation. Binding curves for hydrogen atoms on the 16-carbon rep-

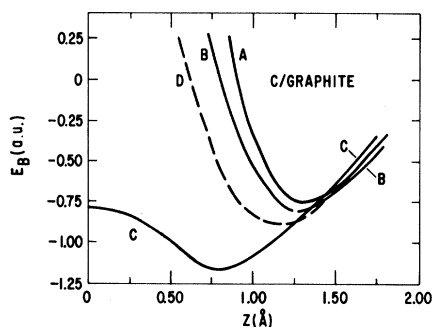


FIG. 5. Binding energy of a carbon adatom (Hartree) as a function of the distance Z above the labeled positions on the 18-C periodically connected lattice.

resentation calculated with the CNDO method yield binding minima of -5.9 eV at 1.50 Å above point A and -3.2 eV at 1.0 Å above point B: These results qualitatively confirm our earlier EHT results as to site preference. CNDO hydrogen results when scaled down by the factor of 5 suggested by the calculated cohesive energy of the graphite substrate are in rough agreement with the EHT results of I. Also there are ~ 0.9 electrons on the adatom, in approximate agreement with the EHT result.

Another example of the effects of the periodic connections on adsorbate-substrate energetics is seen upon the comparison of Fig. 7 with Fig. 9 for the oxygen-atom-graphite system. Indeed, the predicted position of maximum adsorbate stability differs significantly between the surface representation with periodic connection (Fig. 7) and the one without (Fig. 9). A measure of the efficacy of our approximation to periodic boundary conditions is the small difference between the binding curves at C and at C' shown in Fig. 7 for oxygen calculated using the 18-carbon connected representation.

The application of the periodic connections has two effects: saturation of the bonds of the perimeter atoms and introduction of an indirect interaction between the periodically arranged oxygen atoms. Calculations of the binding energy per oxygen atom Z Å above the points C' and C'' indicate the interaction is small. For one adatom per representation, the indirect interaction can be neglected. These results emphasize that the simulation of an extended surface with a finite representation must contain periodic boundary conditions or some suitable form of periodic connection at the edges of the representation.

There is a possible implication of these results with respect to the importance of particle size in heterogeneous catalytic phenomena. It has never been satisfactorily demonstrated whether the increase in catalytic activity with decrease in particle size is due to the increase in surface area, an increase in the number of edge sites which may be responsible for the activity, or the emergence of fundamental differences in chemical reactivity in-

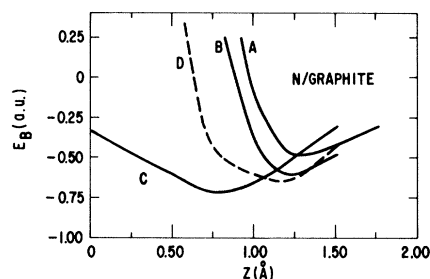


FIG. 6. Binding energy of a nitrogen adatom (Hartree) as a function of the distance Z above the labeled positions on the 18-C periodically connected lattice.

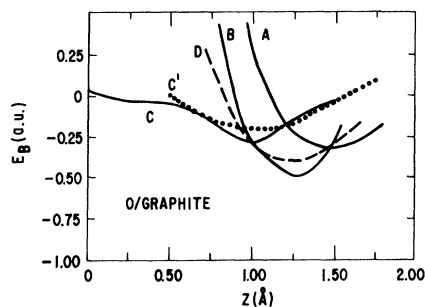


FIG. 7. Binding energy of an oxygen adatom (Hartree) as a function of the distance Z above the labeled positions on the 18-C periodically connected lattice.

trinsic to small irregular particles.

If we drew parallels between small irregularly faceted particles and a representation with no periodic connection, and between a particle with an extended surface and a periodically connected representation, then this difference in calculated adsorbate surface energetics may provide a key ingredient in our understanding of catalytic behavior. Our results for hydrogen and for oxygen on the various representations of the graphite surface demonstrate that fundamental differences in chemical behavior at the surface can indeed be expected between large and extremely small particles.

3. Bonding and Overlap Populations

There are three major points of interest in connection with the bonding and overlap populations associated with the adsorbates. First, more than one surface carbon atom is involved in adatom binding at the position of maximum stability. Second, the greater the magnitude of the overlap population between the adatom and the substrate, the more strongly the adatom is bound to the surface, with hydrogen as the exception. And third, the free valency of the bound adatom varies systematically with the atomic number of the adsorbate. To a large extent, the calculated behavior can be qualitatively rationalized in terms of quantal parameters that characterize the adatom.

A calibration of the atomic overlap population $n(A, B)$ corresponding to single, double, and triple bonds is given by the values of 1.4, 2.1, and 2.5 obtained for H_2 , CO , and N_2 , respectively. The average value of $n(A, B)$ for carbon 9 with its nearest neighbors (Fig. 1) is 1.75, which corresponds to a bond order of ~ 1.3 , as expected. This calibration is useful for the interpretation of the adsorbate overlap populations $n(A)$ [Eq. (2.17)] displayed in Table IV, and in the following discussion.

Hydrogen, in the energetically most stable position (point B, $Z = 1.00 \text{ \AA}$), has the equivalent of a single chemical bond to the lattice. However, this

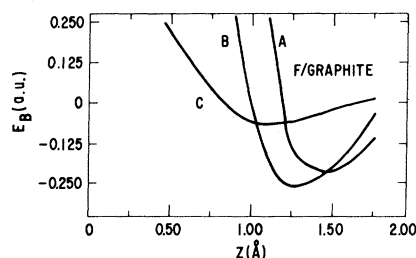


FIG. 8. Binding energy of a fluorine adatom (Hartree) as a function of the distance Z above the labeled positions on the 18-C periodically connected lattice.

single bond consists primarily of two equal contributions from carbon 8 and carbon 9. It is instructive to examine the details of the orbital overlap population between the hydrogen $1s$ orbital and the orbitals of, say, carbon 9. For $\nu = 2s$, $2p_y$, and $2p_z$, $n(1s, \nu) = 0.187$, 0.126 , and 0.403 , respectively. Not only does the hydrogen interact with the π electrons of carbons 8 and 9, but there is a significant interaction with the populations assigned to the σ bond between the two carbons.

The energetically favored binding site of an adatom is expected to be the one with the largest overlap population. The results of Table IV show this is correct, except for hydrogen. The anomalous behavior of hydrogen is due to its ionicity at point C.

There are three species-dependent effects in the series C, N, O, and F that dictate the behavior of these adsorbates on the graphite substrate. The first is the tendency to share with electrons from other sources to form the closed shell $2s^2 2p^6$ configuration: The number of outside electrons needed corresponds to the conventional chemical valencies of 4, 3, 2, and 1, respectively.

Second, the redistribution of electrons of the adatom into the directional lobes responsible for the binding becomes energetically more difficult through the series C, N, O, and F. The energy

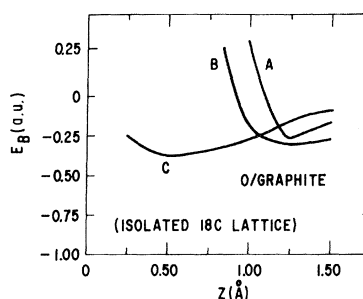


FIG. 9. Binding energy of an oxygen adatom (Hartree) as a function of the distance Z above the labeled positions on an 18-C representation without periodic boundary connections. Compare with Fig. 7. See text.

TABLE IV. Adsorbate overlap populations at binding minima on 18-carbon connected lattice.

Atom	Position ^a			
	A	B	C	D
H	1.07	<u>1.44</u>	1.68	1.26
C	3.35	<u>3.22</u>	<u>4.84</u>	3.17
N	2.55	2.36	<u>3.84</u>	2.23
O	1.04	<u>1.77</u>	1.26	1.51
F	0.67	<u>1.19</u>	0.37	0.92

^aUnderlined values designate most stable binding positions (minimum energy).

of promotion from the 2s to the 2p states increases as may be surmised from the $-\frac{1}{2}(I_{\mu} + A_{\mu})$ values shown in Table I. This effect is offset by the increasing number of p electrons initially available in the series C through F.

The third, and perhaps most decisive, effect is the decreasing diffuseness of the charge distributions associated with the increasing atomic number of the adsorbate. The Slater exponent that characterizes the wave function of the adatoms (Table I) reflects this increasing nuclear charge. The direct result is a decrease in the magnitude of the overlap integrals S_{ij} at constant distance.

The decrease in diffuseness of the orbitals with the increase in atomic number and the need for fewer pairing electrons are responsible for the change in binding-site preference in going from atomic nitrogen to atomic oxygen. Carbon and nitrogen require more electrons for pairing (4 and 3), and their orbitals are sufficiently diffuse to satisfy valency requirements by sharing with a greater number of surface atoms. The major interactions occur between the orbitals of the carbon and nitrogen adatoms and those substrate orbitals that lie in the surface plane. Oxygen and fluorine have more spatially restricted orbitals, require fewer electrons for sharing, and therefore can satisfy the bonding requirements over point B. That is, there is not sufficient overlap with the lattice charge distribution at C to satisfy the bonding requirements. On the basis of this discussion it is not unreasonable to expect that a change in lattice spacing should yield changes in adatom binding-site preferences, as should changes in crystal face.

From the rough calibration made for overlap populations at the beginning of this discussion and the data in Table IV, the number of bonds for hydrogen is ~ 1.0 , adsorbed carbon is ~ 3.3 , nitrogen is ~ 2.4 , oxygen is ~ 1.5 , and fluorine is ~ 0.85 . These values are to be compared with the expected valencies of 1, 4, 3, 2, and 1, respectively. The

unused chemical valency of the first-row adatoms reflects what has been known experimentally for over forty years – chemisorbed adatoms are generally extremely reactive.

IV. SUMMARY

We have shown the CNDO method to be a useful means for the consideration of the interaction of various atomic adsorbates with graphite. In particular, the self-consistent explicit treatment of electron- and core-interaction terms is important in considering the electrophilic adsorbates that could not be treated with the EHT approach. Results have been obtained for both a finite representation of the substrate with periodic boundary connections and for one without these connections. Some significant differences in the calculated chemisorption behavior of small particles and of extended surfaces exist: The implications of this observation are under consideration.

At this stage we can make predictions of binding locations, relative strengths of binding, and charge transfers for a series of atomic adsorbates. This charge transfer is used to make tentative predictions of work-function changes that can occur upon adsorption.

It is important to recognize that the absolute values of the binding energies and the bandwidths obtained are however much too large. In future calculations retention of the overlap matrix in Eq. (2.2) and the adjustment of the parameters used may well ameliorate this condition.

Future treatments of very large adsorbate-substrate separations will certainly require the use of a sum of Slater determinants to describe the system's wave function. Calculations that deal with the dissociation of polyatomic species on a surface must also include such configuration interaction.

Possible changes of lattice-atom positions that may occur upon chemisorption have also been neglected here. For some adsorbate-substrate systems this effect may be very important. However, calculated changes in bond orders and charge distributions for the graphite-lattice atoms upon chemisorption are small (maximum of 15% for lattice bond orders upon adsorption above point B). Thus for graphite with dilute layers of adsorbate this neglect is probably not serious.

In conclusion, it seems apparent that a combination of simple MO and solid-state techniques does hold the promise of allowing the semiquantitative rationalization of physical and chemical behavior at the gas/solid interface.

¹A. J. Bennett, B. McCarroll, and R. P. Messmer, *Surface Sci.* (to be published).

²D. M. News, *Phys. Rev.* **178**, 1123 (1969); T. B. Grimley, *Proc. Phys. Soc. (London)* **90**, 751 (1967);

- 92, 776 (1967); P. Markov and D. Lazarov, *Compt. Rend. Acad. Bulgare Sci.* **22**, 455 (1969); D. Shopov, A. Andreev, and D. Petkov, *J. Catalysis* **13**, 123 (1969); A. Rosenthal and R. Hoffmann (private communication); T. Toya, *J. Res. Inst. Catalysis, Hokkaido Univ.* **8**, 209 (1960); **6**, 308 (1958).
- ³K. Jug, *Theoret. Chim. Acta* **14**, 91 (1969).
- ⁴R. Hoffmann and W. N. Lipscomb, *J. Chem. Phys.* **36**, 2179 (1962).
- ⁵R. Hoffmann, *J. Chem. Phys.* **39**, 1397 (1963).
- ⁶R. Hoffmann, *J. Chem. Phys.* **40**, 2474 (1964).
- ⁷B. J. Duke, *Theoret. Chim. Acta* **9**, 260 (1968).
- ⁸J. A. Pople, D. P. Santry, and G. A. Segal, *J. Chem. Phys.* **43**, S129 (1965).
- ⁹J. A. Pople and G. A. Segal, *J. Chem. Phys.* **43**, S136 (1965).
- ¹⁰J. A. Pople and G. A. Segal, *J. Chem. Phys.* **44**, 3289 (1966).
- ¹¹J. A. Pople and R. K. Nesbet, *J. Chem. Phys.* **22**, 571 (1954).
- ¹²J. A. Pople and D. L. Beveridge, *Approximate Molecular Orbital Theory* (McGraw-Hill, New York, 1970).
- ¹³R. S. Mulliken, *J. Chem. Phys.* **23**, 1833 (1955).
- ¹⁴P. A. Dobosh, Quantum Chemistry Program Exchange, CNINDO: CNDO and INDO molecular orbital program, Indiana University, Program No. 141 (unpublished).
- ¹⁵B. J. Ransil, *Rev. Mod. Phys.* **32**, 239 (1960).
- ¹⁶M. A. Kanter, *Phys. Rev.* **107**, 655 (1957).
- ¹⁷R. P. Messmer and B. McCarroll (unpublished).
- ¹⁸V. S. Fomenko, *Handbook of Thermionic Properties* (Plenum, New York, 1966).
- ¹⁹See F. Bassani and G. Parravicini, *Nuovo Cimento* **50B**, 95 (1967).
- ²⁰T. Delchar and G. Ehrlich, *J. Chem. Phys.* **42**, 2686 (1965).
- ²¹D. P. Stevenson, *J. Chem. Phys.* **23**, 203 (1955).

Grüneisen Parameters of the Alkali Halides*

R. Ruppin† and R. W. Roberts

Department of Physics, University of North Carolina, Chapel Hill, North Carolina 27514

(Received 21 August 1970)

The microscopic Grüneisen parameters of 13 alkali halides have been calculated over the entire Brillouin zone by solving the lattice dynamical problem at different pressures. A six-parameter shell model has been used and the variation of the parameters with pressure was deduced from the pressure dependence of the three elastic constants, of the two dielectric constants, and of the infrared absorption frequency. The quasi-harmonic-model values of the macroscopic Grüneisen parameter at 295°K were obtained by appropriate averaging over the microscopic mode gammas. The results are in good agreement, but are systematically larger than Grüneisen parameters deduced from thermal-expansion data.

I. INTRODUCTION

The Grüneisen parameter¹ of a solid is defined by the relation

$$\gamma_G = V\beta B_T / C_V \quad (1)$$

in terms of macroscopic variables: β - the coefficient of volume expansion, V - the volume, C_V - the specific heat at constant volume, and B_T - the isothermal bulk modulus. On the other hand, within the quasi-harmonic approximation, the Grüneisen parameter can be expressed in terms of the microscopic Grüneisen parameters (mode gammas) defined by

$$\gamma_i = - \frac{d \ln \omega_i}{d \ln V}, \quad (2)$$

where ω_i is the frequency of the i th normal mode. Although γ_G values for many alkali halides are known, a systematic interpretation in terms of microscopic variables has not been given to our knowl-

edge.

The results of measurements of the pressure dependence of the elastic constants have been used in the past to calculate the mode gammas of the low-frequency acoustic modes from

$$\gamma_i = - \frac{1}{6} + \frac{B_T}{2C_i} \left(\frac{\partial C_i}{\partial P} \right)_T, \quad (3)$$

where C_i is the appropriate elastic constant. The Grüneisen parameter has been estimated by averaging over these acoustic mode gammas.²⁻⁴ Such a procedure is justified at low enough temperatures at which only the nondispersive acoustic modes are excited. It fails in principle, however, at higher temperatures, where dispersive acoustic modes as well as optical modes begin to contribute, and should be replaced by a detailed lattice dynamical calculation.

Arenstein *et al.*⁵ have calculated the mode gammas of NaCl from the rigid-ion model with nearest-neighbor forces only, using a perturbation method.